

## Supporting Information

# Facile Approach to the Synthesis of Carbon Nanodots and their Peroxidase Mimetic Function in Azo Dyes Degradation

Afsaneh Safavi\*, Fatemeh Sedaghati, Hamidreza Shahbaazi, Elaheh Farjami

### Experimental details

1-Iodoctane, pyridine, diethyl ether, hydrogen peroxide, methyl red (MR) and methyl orange (MO) were acquired from Merck.  $\text{NH}_4\text{PF}_6$  and Quinine sulfate were supplied by Fluka. *N*-Octylpyridinium hexafluorophosphate ( $\text{OPPF}_6$ ) was synthesized as previously reported.<sup>22</sup>

Synthesis of carbon Nanodots was done using domestic microwave oven (Delonghi, type MW 665 in the combined microwave/fan-oven mode). A desired amount of ionic liquid (IL) (about 50 mg) was placed in a test tube and was heated in a microwave oven (Power,  $P = 450 \text{ W}$ ) for approximately 2 min. The color change of IL ( $\text{OPPF}_6$ ) from colorless to yellow, and finally, to dark brown, which signifies the production of CDs is shown in **Figure S1**. 4 mL of distilled water was added to the test tube and sonicated in an ultrasonic bath for 3 min. A colorless carbon nanodots (CDs) solution was obtained following ultra-filtration of the dark brown suspension through a  $0.2 \mu\text{m}$  filter membrane. Absorbance, FTIR and photoluminescence (PL) spectra were recorded using a Perkin-Elmer Lambda 2 spectrophotometer, Shimadzu FT-IR 8300 spectrometer, a Perkin-Elmer LS-55 luminescence spectrometer, respectively. Images of solutions were taken by a CCD camera (Canon EOS D30). FTIR spectra are shown in **Figure S2**. XPS Spectra were recorded using a Kratos Axis UltraDLD instrument (Kratos Ltd, Telford, UK)

equipped with a monochromated aluminium anode (Al  $k\alpha$  1486 eV) operating at 45 W power (15 kV and 3 mA) with pass energies of 40 eV for high resolution and 160 eV for wide scan. XPS spectrum of CDs is shown in **Figure S3**. A three-dimensional image of synchronous fluorescence data of CDs solution is shown in **Figure S4**.

The photoluminescence intensity of the as-synthesized CDs was stable at pH range of 4 – 9 (Figure. S5).

A typical luminescence lifetime was also measured by FLS920 spectrometer with time correlated single photon counting. The PL decay of the CDs was deconvoluted using a mono-exponential decay function to yield a lifetime of 6.7 ns (**Figure S6**).

The quantum yield of CDs depends on the fabrication method and their surface chemistry. The quantum yield of CDs with blue emission was estimated against quinine sulfate (QS) in 0.1M H<sub>2</sub>SO<sub>4</sub> ( $\lambda_{\text{ex}}$ =330nm, literature  $\Phi_{\text{F}}$ = 0.54). Quinine sulfate was dissolved in 0.1M H<sub>2</sub>SO<sub>4</sub> (refractive index ( $\eta$ ) of 1.33) and the CDs were dissolved in distilled water ( $\eta$ =1.33). The following equation was employed for  $\Phi_{\text{F}}$  calculation.

$$\phi = \phi_R \times \frac{I}{I_R} \times \frac{A_R}{A} \times \frac{\eta^2}{\eta_R^2}$$

where  $\Phi$  is the quantum yield (QY),  $I$  is the measured integrated emission intensity,  $\eta$  is the refractive index, and  $A$  is the absorbance. The subscript R refers to the reference fluorophore of known quantum yield. The  $I/A$  for the quinine sulfate (reference fluorophore) and CDs were obtained from the slope of the curve a and b in **Figure S7**

which are equal to  $2 \times 10^{-6}$  and  $1 \times 10^{-6}$ , respectively. The quantum yield (QY) was calculated to be 27% .

The optical band gap energy of the CDs was also calculated by plotting  $(\alpha h\nu)^2$  versus  $h\nu$ . **(Figure S8).**

HRTEM images were recorded on an electronic microscopy (Tecnai F20- 200KV).

X-Ray diffraction (XRD) pattern was obtained by using a D8 ADVANCE type (BRUKER-Germany) with Cu-K $\alpha$  radiation ( $\lambda = 0.1542$  nm) **(Figure S9).**

For degradation studies, a sample containing  $10.0 \text{ mg L}^{-1}$  of methyl red in universal buffer pH=10 was placed in a quartz cell. The reaction was initiated by adding a known dose of  $\text{H}_2\text{O}_2$  (160 mM) to the solution held at a constant temperature ( $T = 25^\circ \text{C}$ ). The amount of methyl red in the reaction was quantified through the measurement of the decay of absorbance at maximum wavelength (425 nm) as a function of time. The kinetic parameter of MR degradation was obtained by the first-order model. The value of the rate constant and the degradation efficiency of MR after 200 min were  $9.5 \times 10^{-3} \text{ min}^{-1}$  and 83%, respectively while these values for solution in the absence of CDs were  $2.2 \times 10^{-4} \text{ min}^{-1}$  and 4.5%. The results showed that the rate constant for MR is 43 times more than that in the absence of CDs suggesting very good catalytic activity of CDs. The images of solutions after degradation are shown in **Figure S10**. Degradation of the dyes in the absence of oxidant and in the presence of CDs in sunlight was also studied **(Figure S11)**. The same procedure was repeated for MO degradation study ( $\lambda_{\text{max}} = 462$  nm). The kinetic parameter of MO degradation was obtained by the first-order model. The values of  $7.7 \times 10^{-3} \text{ min}^{-1}$  and 76% were evaluated for rate constant and the degradation

efficiency of MO in the presence of CDs, respectively. These values were as  $1.13 \times 10^{-3}$   $\text{min}^{-1}$  and 15%, respectively in the absence of CDs (**Figure S12**).

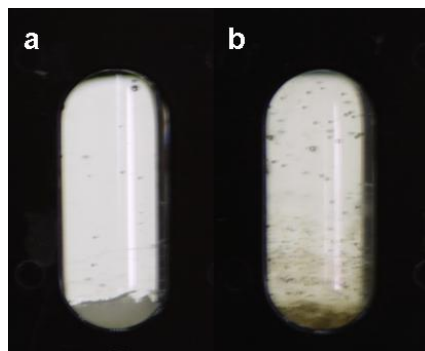


**Figure S1.** Images of OPPF<sub>6</sub> a) before and b) after applying MW.

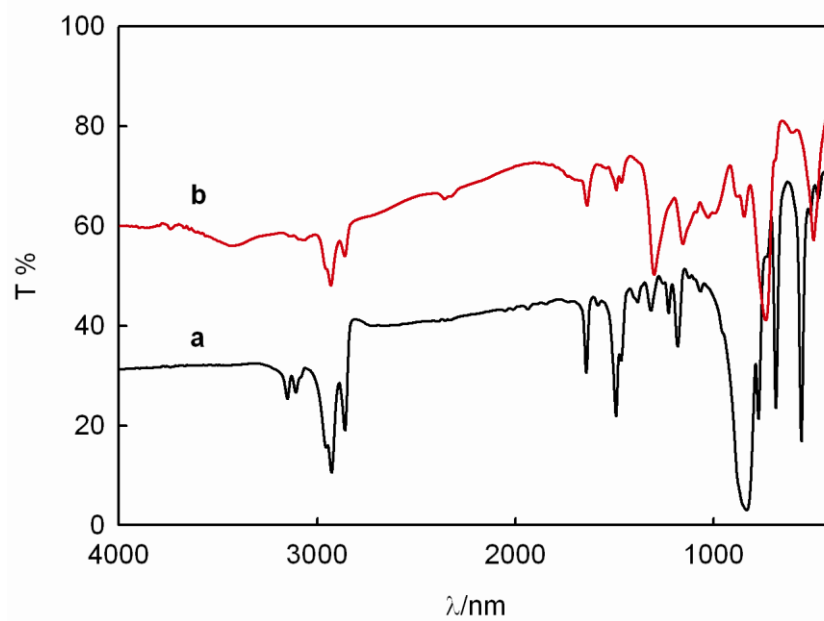


**Figure S2.** FTIR spectra of OPPF<sub>6</sub> a) before and b) after applying MW.

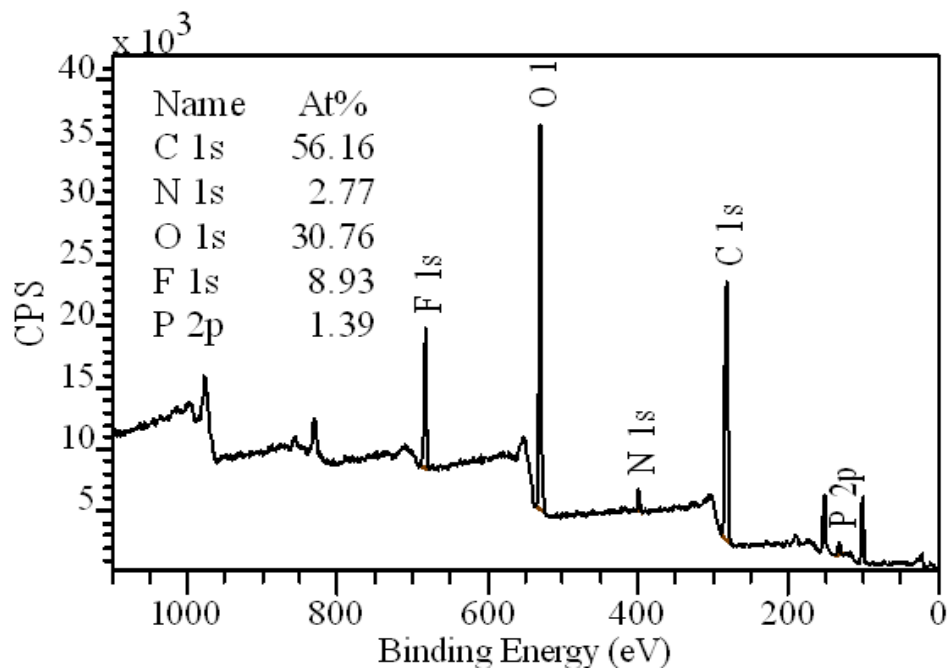


**Figure S3.** XPS spectrum of CDs.

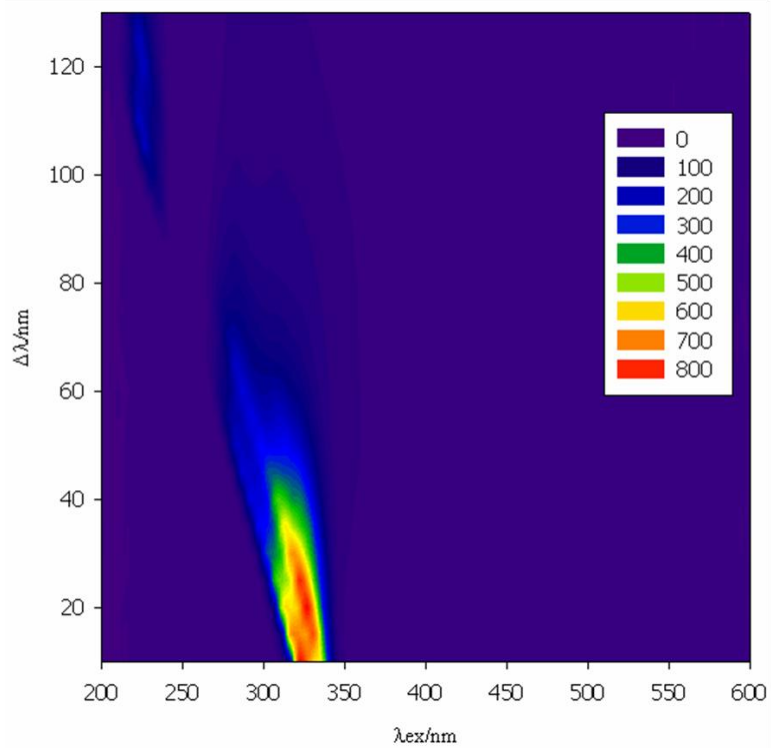


**Figure S4.** 3D synchronous PL responses of CDs solution

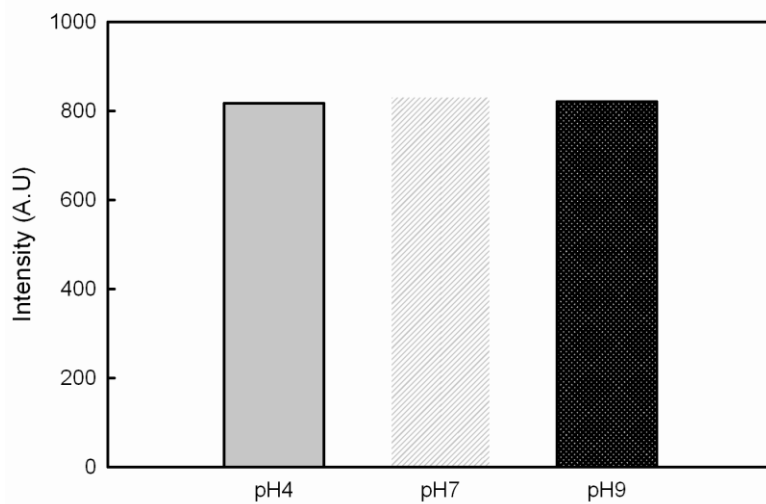


**Figure S5.** Effect of pH on PL intensity of CDs solution.

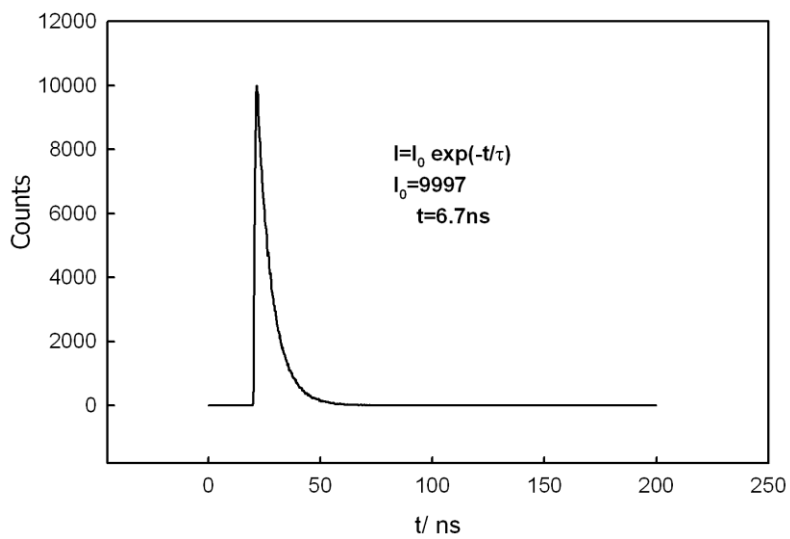


**Figure S6.** Fluorescence decay time profile of CDs.



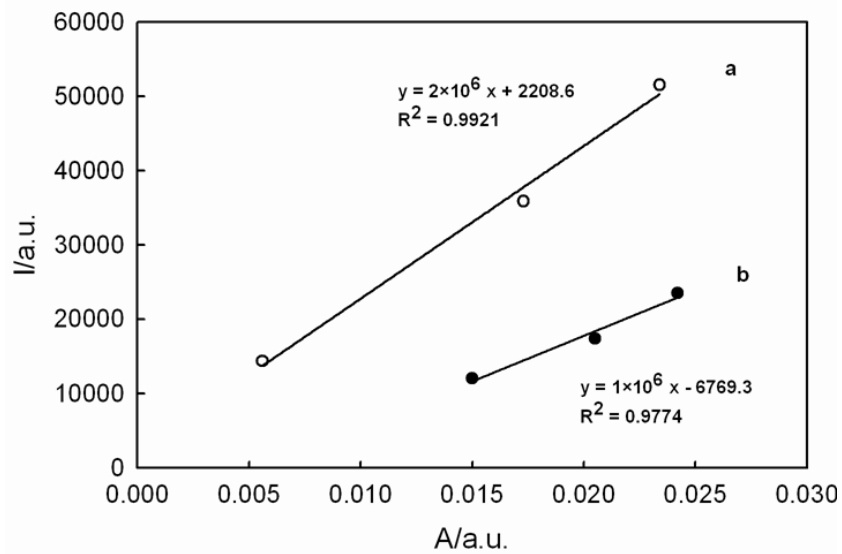


**Figure S7.** Integrated intensity v.s absorbance a) quinine sulfate b) CDs solution.

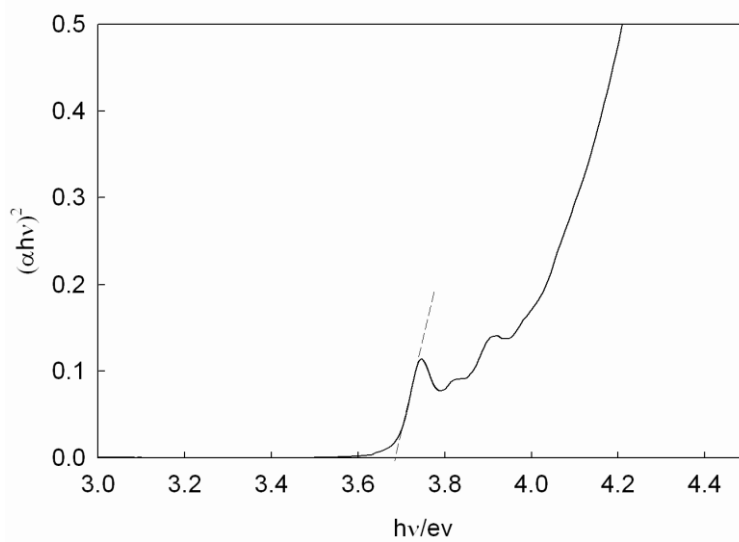


**Figure S8.** Plotting of  $(\alpha hv)^2$  versus  $hv$  for optical energy band gap calculation for CDs.

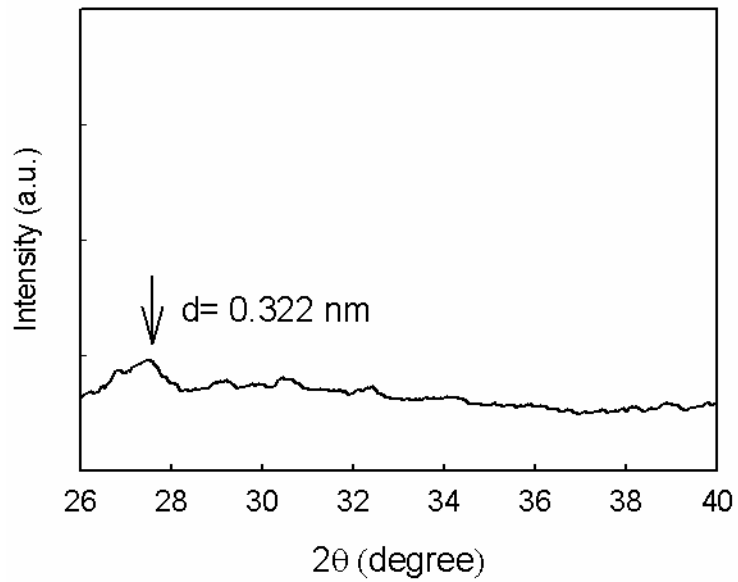


**Figure S9.** XRD pattern of CDs.

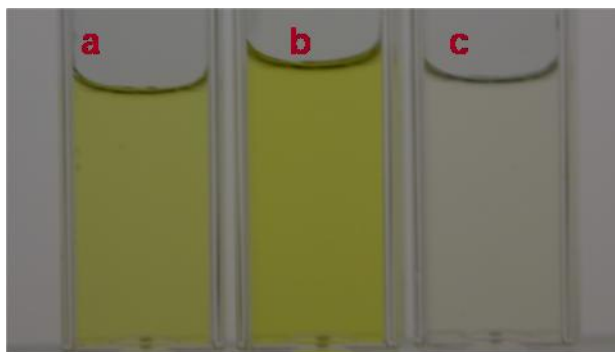


**Figure S10.** Change in the color of solution after 200 min of the reaction of MR with  $\text{H}_2\text{O}_2$  (160 mM) (a) only in buffer pH=10 (b) in blank IL solution at pH=10 and (c) in the presence of CDs at pH=10.

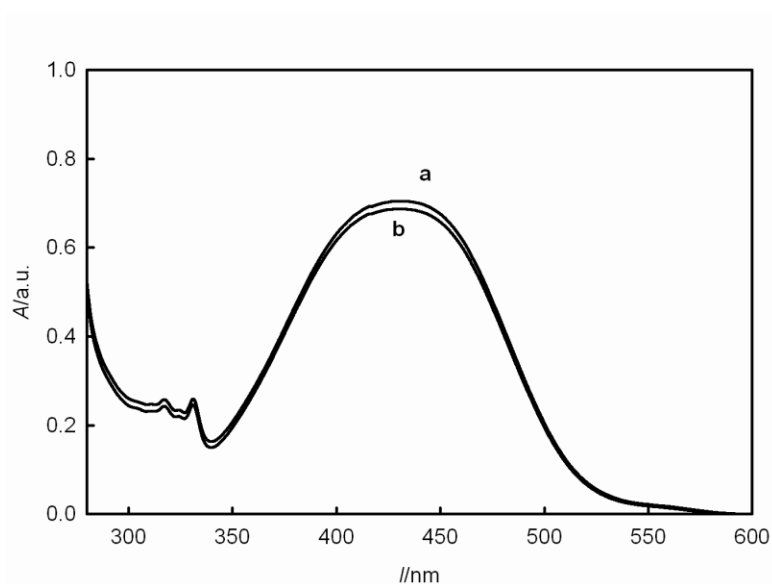


**Figure S11.** Degradation of MR in pH=10 in presence of CDs and the absence of oxidant after 200 min a) room light b) sunlight.

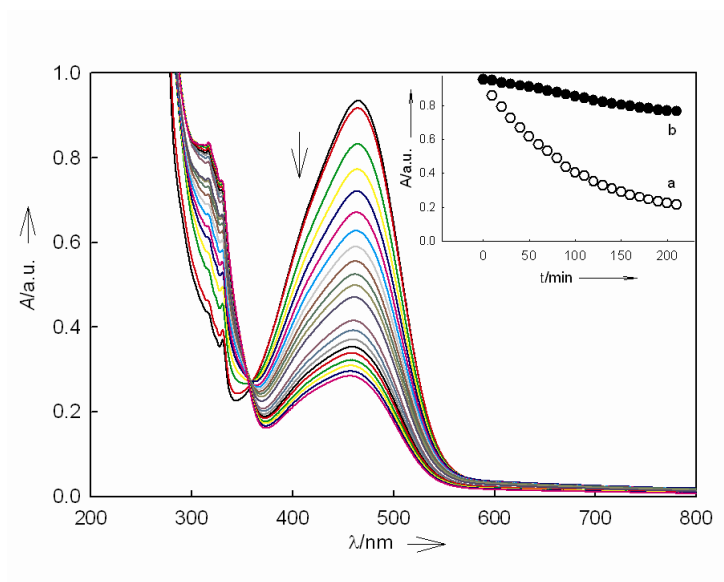


**Figure S12.** Change in the absorbance spectrum, with time, during the reaction of MO with H<sub>2</sub>O<sub>2</sub> (160 mM) in the presence of CDs (pH=10). Inset shows comparison of absorbance decay with time, (a) in the presence and (b) in the absence of CDs.